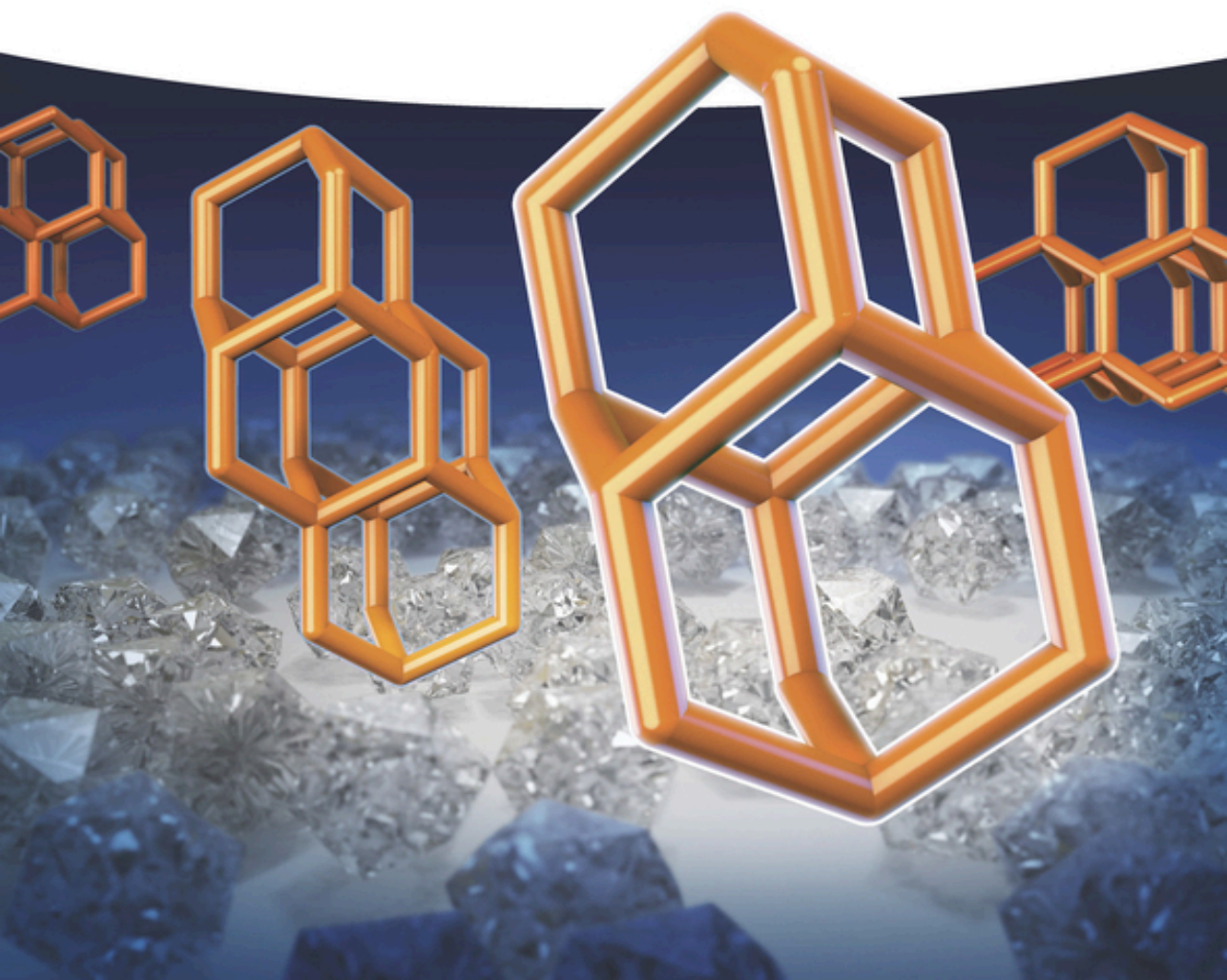


WILEY-VCH

Andrey A. Fokin, Marina Šekutor,
and Peter R. Schreiner

The Chemistry of Diamondoids

Building Blocks for Ligands, Catalysts,
Materials, and Pharmaceuticals



The Chemistry of Diamondoids

The Chemistry of Diamondoids

Building Blocks for Ligands, Catalysts, Materials,
and Pharmaceuticals

Andrey A. Fokin

Marina Šekutor

Peter R. Schreiner

Authors

Prof. Dr. Andrey A. Fokin

Igor Sikorsky Kyiv Polytechnic Institute
Department of Organic Chemistry
Beresteiskyi Ave. 37
03056 Kiev
Ukraine

Dr. Marina Šekutor

Ruđer Bošković Institute
Department of Organic Chemistry and
Biochemistry
Bijenička 54
10 000 Zagreb
Croatia

Prof. Dr. Peter R. Schreiner

Justus Liebig University
Institute of Organic Chemistry
Heinrich-Buff-Ring 17
35392 Giessen
Germany

Cover Image: © Formgeber, Mannheim

■ All books published by **WILEY-VCH** are carefully produced. Nevertheless, authors, editors, and publisher do not warrant the information contained in these books, including this book, to be free of errors. Readers are advised to keep in mind that statements, data, illustrations, procedural details or other items may inadvertently be inaccurate.

Library of Congress Card No.: applied for

British Library Cataloguing-in-Publication Data

A catalogue record for this book is available from the British Library.

Bibliographic information published by the Deutsche Nationalbibliothek

The Deutsche Nationalbibliothek lists this publication in the Deutsche Nationalbibliografie; detailed bibliographic data are available on the Internet at <<http://dnb.d-nb.de>>.

© 2024 WILEY-VCH GmbH, Boschstr. 12, 69469 Weinheim, Germany

All rights reserved (including those of translation into other languages). No part of this book may be reproduced in any form – by photoprinting, microfilm, or any other means – nor transmitted or translated into a machine language without written permission from the publishers. Registered names, trademarks, etc. used in this book, even when not specifically marked as such, are not to be considered unprotected by law.

Print ISBN: 978-3-527-34391-1

ePDF ISBN: 978-3-527-81294-3

ePub ISBN: 978-3-527-81293-6

oBook ISBN: 978-3-527-81295-0

Typesetting: Straive, Chennai, India

Contents

Preface	<i>ix</i>
Abbreviations	<i>xi</i>
Acknowledgments	<i>xv</i>
Author Biographies	<i>xvii</i>
1	Description of Diamondoids 1
1.1	Nomenclature 2
1.2	Strain 5
1.3	Preparation of Diamondoids 8
1.4	Physical Properties of Diamondoids 14
1.5	Spectroscopy of Diamondoids 18
1.6	Ionization Potentials 23
1.7	Electron Affinities 24
1.8	Vibrational Spectroscopy 25
	References 28
2	Naturally Occurring Diamondoids 35
2.1	Diamondoid Occurrence in the Earth's Crust 38
2.2	Diamondoids in Geochemical Studies 40
2.3	Diamondoid Formation in the Earth's Crust 42
2.4	Large-scale Isolation of Natural Diamondoids 44
2.5	Alternative Natural Sources of Diamondoids 48
2.6	Other Diamondoid Derivatives in Nature 50
	References 52
3	Diamondoids as Alkane CH Activation Models 63
	References 69
4	Preparative Diamondoid Functionalizations 75
4.1	Halogenations 75
4.2	Diamondoid Alcohols and Ketones 83
4.3	Carboxylic Acids and Their Derivatives 98
4.4	Nitrogen-Containing Compounds 103

- 4.5 Phosphorous- and Sulfur-Containing Compounds 108
- 4.6 Single Electron Oxidations of Diamondoids 113
- 4.7 Other Diamondoid Derivatives 118
- References 121

- 5 Diamondoid Self-Assembly 137**
- 5.1 Adamantane-Containing SAMs on Surfaces 137
- 5.2 Higher Diamondoids for SAM Formation 146
- 5.3 Pristine Diamondoids on Surfaces 157
- 5.4 Other Applications of Diamondoid SAM Materials 157
- 5.5 Adamantane-stabilized Metal Nanoparticles 160
- References 162

- 6 Growing Diamond Structures from Diamondoids Via Seeding 171**
- 6.1 Diamondoid-Promoted Growth of Diamond Under HT-HP or CVD Conditions 171
- 6.2 Higher Diamondoids for Diamond Nucleation 177
- 6.3 Diamond Growth Inside Nanotubes 180
- References 186

- 7 Diamondoid Polymers 193**
- 7.1 Polymers Based on 1-Adamantyl-1-adamantane (1ADAD) 194
- 7.2 Polymers Based on Monofunctionalized Diamantanes 197
- 7.3 Polymers Based on Difunctionalized Diamantanes 199
- References 207

- 8 Diamondoids in Catalysis 213**
- References 232

- 9 Medicinal Compounds 239**
- References 245

- 10 Supramolecular Architectures 251**
- References 270

- 11 Diamondoid Oligomers 279**
- 11.1 Saturated Diamondoid Oligomers 279
- 11.2 Unsaturated Oligomers 287
- References 293

- 12 Doped Diamondoids 305**
- 12.1 @-Doping 306
- 12.2 Internal Doping 308

12.3	External Doping	318
	References	329
13	Perspective	339
	References	340
	Index	343

Preface

Diamondoids are a prominent and large family of nanoscale hydrocarbons that are composed of carbon atoms arranged in a cubic diamond lattice structure. These molecules range in size from ten (adamantane) to several dozen carbon atoms and have unique properties that make them valuable for a large variety of applications. Since the discovery of diamondoids in petroleum deposits in the 1930s, they have been studied extensively, and their potential for use in materials science, nanotechnology, and medicine has been explored.

The origin of diamondoids can be traced back to the geological processes that create petroleum deposits. Petroleum formed from the remains of ancient (marine) organisms, which are buried deep underground and subjected to high temperatures and pressures over millions of years. During this process, some of the carbon in the organic matter transforms into diamondoids because they constitute the thermodynamically most stable hydrocarbons.

In recent decades, researchers have also discovered that diamondoids beyond adamantane can be synthesized in the laboratory using a variety of methods, including chemical vapor deposition, solution-phase synthesis, and high-pressure, high-temperature techniques. This has opened up new avenues for research and development, as they can be tailored to have specific properties and functionalities that are not found in natural diamondoids.

Even though the parent diamondoid, adamantane, was discovered in petroleum as early as 1933, it was not until the 1970s that researchers started to study these molecules in earnest. Advances in synthetic accessibility, analytical techniques, and computational modeling have since enabled us to study the properties and behavior of diamondoids in detail, leading to a better understanding of their potential applications. For example, their exceptional thermodynamic stability and mechanical strength make them ideal for use in nanoscale electronic devices, such as rectifiers and electron emitters. Additionally, their biocompatibility and low toxicity make diamondoid derivatives attractive candidates for use in pharmaceutical applications. Furthermore, diamondoids have been proposed as building blocks for the construction of new materials, such as diamond-like nanowires and coatings.

This comprehensive book on diamondoids aims to provide a thorough overview of the current state of research on these fascinating molecules. It covers a wide range of topics, from the synthesis and characterization of diamondoids to their applications

in various fields. The book is divided into several sections, each focusing on a different aspect of diamondoid research.

The first chapter introduces the basic concepts of diamondoid chemistry, including their structures, nomenclature, (spectroscopic) properties, and synthesis. It covers the various methods to synthesize diamondoids, including techniques that also help understand how they abundantly form in nature. The strain energies of increasingly larger diamondoids are also assessed to aid in this endeavor.

The second section of the book focuses on naturally occurring diamondoids and the role they play in the petroleum industry and in geosciences. Ways for their formation also are described including man-made approaches to prepare them on a large scale.

The third and fourth chapters cover C—H-bond functionalization, as this is a precondition for their use in many applications. As diamondoids are alkanes with strong and multiple, similarly reactive C—H-bonds, this is an exercise in practically applicable and scalable methods for alkane functionalization. This also enables the fine-tuning of the diamondoid properties, as they react sensitively to substitution.

Chapters 5–12 are devoted to the applications of (functionalized) diamondoids, including self-assembly, growing diamonds from diamondoids via seeding, polymers, supramolecular architectures, diamondoid oligomers, and doped diamondoids. The applications in catalysis and as medicinal compounds are also outlined to demonstrate the huge and, for the most part, untapped potential these building blocks offer.

We close by providing a brief perspective on where diamondoids could continue to leave their mark and what future directions in diamondoid research might entail. We hope to provide a thorough overview of the current state of research on these fascinating molecules and to highlight their potential for use in a wide range of applications.

February 2024

Andrey A. Fokin
Marina Šekutor
Peter R. Schreiner

Abbreviations

6-31G(d,p)	split-valence basis sets with d and p polarization functions on the heavy atom and on hydrogen, respectively
AFM	atomic force microscopy
AIBN	azobis(isobutyronitrile)
AIM	atoms-in-molecules
B3LYP	Becke 3-parameter Lee–Yang–Parr exchange-correlation DFT functional
B3LYP-D3	Becke 3-parameter Lee–Yang–Parr exchange-correlation DFT dispersion-corrected functional
cc-pVDZ	double-zeta correlation-consistent basis set
cc-pVTZ	triple-zeta correlation-consistent basis set
CB	cucurbituril
CD	cyclodextrin
CNT	carbon nanotube
CVD	chemical vapor deposition
DAST	diethylaminosulfur trifluoride
DBD	dielectric barrier discharge
DED	dispersion energy donor
DFT	density functional theory
DMSO	dimethyl sulfoxide
DMF	dimethyl formamide
EA	electron affinity
EAS	Engler–Andose–Schleyer (force field)
ECEC	electron transfer-chemical reaction-electron transfer-chemical reaction
EOM	equation of motion
EPD	electronic photodissociation
ESI	electrospray ionization
FWHM	full-width half-max
GCD	graphite-cluster diamond
GC–GC-TOFMS	2D gas chromatography coupled with time-of-flight mass spectrometry
GC–MS	gas chromatography coupled with mass spectrometry

GC-MS/MS	gas-chromatography-tandem mass spectrometry
GOR	gas/oil ratio
HCET	H-coupled electron transfer
HOMO	highest occupied molecular orbital
HPLC	high-performance liquid chromatography
HT-HP	high temperature and high pressure
IETS	inelastic electron tunneling spectroscopy
IP	ionization potential
IR	infrared
IRPD	infrared photodissociation
IR-STM	infrared scanning tunneling microscopy
ITO	indium-tin oxide
IUPAC	International Union of Pure and Applied Chemistry
JT	Jahn-Teller
KIE	kinetic isotope effect
LD	London dispersion
LUMO	lowest unoccupied molecular orbital
MALDI	matrix-assisted laser desorption ionization
MANSE	microwave-assisted nonionic surfactant extraction
MD	molecular dynamics
MP	microwave plasma
MP2	Møller-Plesset second-order perturbation
NAPS	non-aqueous phase pollution liquids
NEA	negative electron affinity
NEXAFS	near-edge X-ray absorption fine structure
NHPI	<i>N</i> -hydroxyphthalimide
NMR	nuclear magnetic resonance
PBE	Perdew-Burke-Ernzerhof exchange DFT functional
PINO	phthalimide- <i>N</i> -oxyl (radical)
PTC	phase-transfer catalysis
PMC	polymethacrylate
R_o	vitritite reflectance
SAM	self-assembled monolayer
SCX	single crystal X-ray
SET	single-electron transfer
SOMO	single-occupied molecular orbital
SWCNT	single-wall carbon nanotube
TBDMS	<i>tert</i> -butyldimethylsilyl
TBHP	<i>tert</i> -butylhydroperoxide
TCB	tetracyanobenzene
TD	time-dependent
TEM	transmission electron microscopy
TFA	trifluoroacetic acid
TGA	thermogravimetric analysis
TMAD	tetramethyl adamantane

TOF	time-of-flight
TPPE	two-photon photoemission
TSR	thermochemical sulfate reduction
UHV	ultrahigh vacuum
UV	ultraviolet
X-PEEM	X-ray photoemission electron microscopy
XPS	photoelectron microscopy

Acknowledgments

Our work on diamondoids was supported through exchanges with many very knowledgeable and helpful colleagues, including, *inter alia*, Robert M.K. Carlson, Jeremy E.P. Dahl, Matthew A. Gebbie, Jean-Cyrille Hierso, Nicholas A. Melosh, Thomas Möller, Hisanori Shinohara, Z.-X. Shen, and Trevor Willey.

Even more importantly, we are grateful to our many co-workers who have executed all the work on diamondoids both experimentally and computationally. We are deeply indebted to their dedication, hard work, and inspiration.

Finally, this work was generously supported by the Alexander von Humboldt Foundation, the Bundesministerium für Bildung und Forschung, the Deutsche Forschungsgemeinschaft, the Fonds der Chemischen Industrie, the German Academic Exchange Service, the Ministry of Education of Ukraine, the NATO Science Program, the Ukrainian Basic Research Fund, the US Department of Energy, and the Volkswagen Foundation.

Author Biographies



Andrey A. Fokin is currently Head of the Department of Organic Chemistry and Technology at National Technical University “Igor Sikorsky Kiev Polytechnic Institute,” Ukraine. He studied chemistry at the Kiev Polytechnic Institute, where he received the degrees of Candidate of Chemical Sciences (1985) in diamondoid chemistry under the supervision of Prof. Pavel A. Krasutsky and Doctor of Chemical Sciences in pesticide chemistry and technology (1995). He was a DAAD (1996) and Alexander von Humboldt (1997–1998) research fellow in the groups of Prof. P. v. R. Schleyer at the University of Erlangen-Nürnberg and Prof. P. R. Schreiner at Göttingen University (Germany). He has been a visiting professor at the universities of Minnesota and Georgia (USA) as well as in Giessen (Germany). His research mostly concentrates on the combination of computational and experimental studies with applications in organic, physical-organic, medical, agricultural chemistry, and nanotechnology and has been published in over 200 peer-reviewed papers and books.



Marina Šekutor is currently a senior research associate at the Ruđer Bošković Institute, Zagreb, Croatia. She was born in 1986 in Zagreb and received her B.Sc.Eng. degree in 2008 and PhD (under the mentorship of Prof. Kata Majerski) in 2013, both from the Faculty of Science, University of Zagreb. She obtained a Humboldt postdoctoral fellowship (research in the Schreiner group, 2015–2017) and upon returning to Zagreb continued to pursue her interests in the chemistry of diamondoids. M. Šekutor received the annual award to young scientists and artists in 2014, the annual award of the Ruđer Bošković Institute in 2017, and the award for organic chemistry “Vladimir Prelog” in 2019 (awarded by the Croatian Chemical Society). She has been a visiting scientist at the University of Maryland, USA, and is a lecturer at the Faculty of Science, University of Zagreb, and the Faculty of Medicine, Josip Juraj Strossmayer

University of Osijek. She is a Croatian Chemical Society member, where she currently holds the position of Secretary from 2021, and a Croatian Humboldt-Club member. Her research interests include supramolecular host–guest chemistry of polycyclic compounds, cluster assemblies in helium nanodroplets driven by London dispersion, and use of diamondoid derivatives in materials science.



Peter R. Schreiner is professor of organic chemistry and Liebig-Chair at the Institute of Organic Chemistry at the Justus Liebig University Giessen, Germany. He studied chemistry in his native city at the University of Erlangen-Nürnberg, Germany, where he received his Dr. rer. nat. (1994) in organic chemistry. Simultaneously, he obtained a PhD (1995) in computational chemistry from the University of Georgia, USA. He completed his habilitation (assistant professorship) at the University of Göttingen (1999) before becoming associate professor at the University of Georgia (Athens, USA) and head of the institute in Giessen in 2002. P. R. Schreiner is an elected member of the Leopoldina – German National Academy of Sciences, the North Rhine-Westphalian Academy of Sciences, Humanities, and the Arts, the Academy of Science and Literature (Mainz), the Berlin-Brandenburg Academy of Sciences, and is a Fellow of the Royal Society of Chemistry. He received the Dirac Medal (2003, WATOC), the Adolf-von-Baeyer Memorial Award of the German Chemical Society in 2017, the RSC Award in Physical Organic Chemistry of the RSC in 2019, the Academy Award of the Berlin-Brandenburg Academy of Science in 2020, the ACS Arthur C. Cope Scholar Award in 2021, and the Gottfried–Wilhelm–Leibniz–Award 2024 of the German Research Council (DFG). He has been a visiting professor at the CNRS in Bordeaux, the Technion in Haifa, the Australian National University in Canberra, and the University of Florida in Gainesville. His research interests include organic reaction dynamics and reactive intermediates, quantum mechanical tunneling, as well as London dispersion interactions as probed in the realm of nanodiamonds and organocatalysis.

1

Description of Diamondoids

Shortly after the 3D structure of diamond was determined, the German chemist Hermann Decker recognized the connection between diamond and saturated hydrocarbons with “the 6-ring system built out into the third dimension” and suggested the term “diamondoid” for such molecules [1]. As the spatial arrangement of the carbon atoms resembles the diamond crystal lattice, diamondoids can therefore be viewed as hydrogen-terminated nanometer-sized diamonds with distinctive properties determined by their sizes and topologies. The smallest diamondoid is adamantane (**AD**, Figure 1.1), which has a cage skeleton consisting of ten carbons. Formal addition of further isobutyl fragments to the **AD** parent structure in a cyclohexane ring-forming manner results in higher diamondoid homologues. Diamondoids are classified as lower and higher homologues: lower diamondoids have only one isomeric form and include **AD** ($C_{10}H_{16}$), diamantane (**DIA**, $C_{14}H_{20}$), and triamantane (**TRIA**, $C_{18}H_{24}$), while higher diamondoids start with tetramantane (**TET**, $C_{22}H_{28}$) and possess isomers. Among three possible **TET** isomers, one is chiral (**123TET**) and is viewed as the parent of a new family of σ -helicenes [2]. As the cage grows, the number of isomers increases and beginning from pentamantane (**PENT**) spreads into different molecular weight subgroups, i.e., **PENT** has nine isomers with the $C_{26}H_{32}$ formula and one isomer with the $C_{25}H_{30}$ formula. Some other hydrocarbons also satisfy the structural criteria of partial or complete superposition on the diamond lattice, e.g., cyclohexane and decalin, so diamondoids are more precisely defined as “hydrocarbons containing at least one adamantane unit wholly or largely superimposable on the diamond lattice” [3]. Due to this definition, higher diamondoids bridge the gap between saturated hydrocarbons and diamond and are sometimes called nanodiamonds (in plural form to differentiate them from heterogeneous mixtures of nanodiamond material obtained by chemical vapor deposition, detonation, or shock-wave techniques [4]).

The molecular symmetry of diamondoids also plays a role in their self-assembly, readily producing crystals or serving as nucleation centers for bigger nanomaterial architectures. The smallest diamondoid **AD** is highly symmetric (T_d point group), whereas symmetry is generally (but not always) reduced as the diamondoids become larger, e.g., **DIA** and **TRIA** belong to the D_{3d} and C_{2v} point groups, respectively.

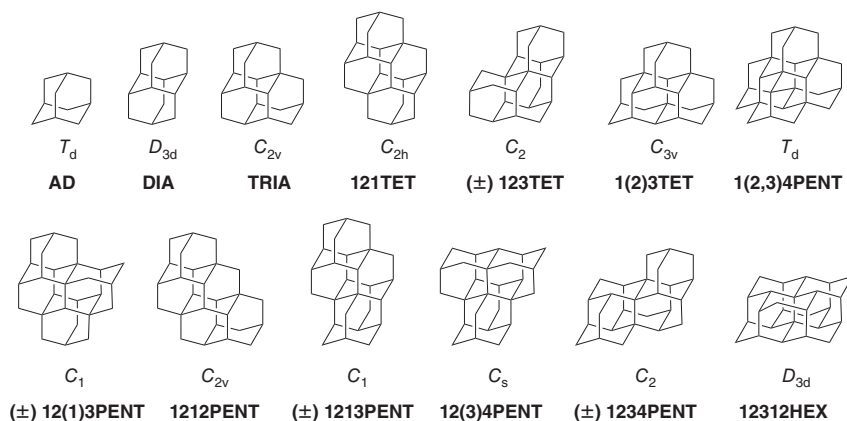


Figure 1.1 Structures and symmetry of diamondoid homologues up to cyclohexamantane (**12312HEX**).

Isomers of the first higher diamondoid **TET** display C_{2h} (**121TET**), C_2 (**123TET**), and C_{3v} (**1(2)3TET**) symmetry (Figure 1.1).

Note that **TETs** exemplify a common occurrence for higher diamondoids: different isomers have markedly different symmetries, which can be useful in material design by tailoring both the solubility of the material and the shape of the used building blocks. Moreover, diamondoids have one important advantage over bulk diamonds: they are “knowable,” that is, their shapes are precisely determined by their molecular structure (rods, disks, helices, prisms, pyramids, cubes, etc.; Figure 1.2) and stoichiometry, and they can be obtained in homogeneous forms because they are single-molecule, nanometer-scale-sized building blocks. For instance, **DIA** and **121TET** are rod-shaped nanodiamond particles, **TRIA** and **1212PENT** have triangular shape, **1(2,3)4PENT** and **1231241(2)3DEC** are tetrahedron and cube, respectively, and **1(2)3TET** and **12312HEX** are prisms.

According to the definition of polymantanes, face-fused **AD** cage structures that are the focus of this book are not the only existing diamondoids. For example, **AD** dimers and higher single-bonded oligomers also belong to the class of diamondoid hydrocarbons (Figure 1.3). The first step in determining whether a saturated hydrocarbon belongs to the class of polymantane compounds is to check whether it has at least one **AD** subunit. If yes, then the next condition is that all cage atoms of the molecule need to be part of an **AD** unit; if that is also true, then the final condition is that two or more **AD** cages need to have at least six common carbon atoms, meaning that they share one face. When these conditions are met, a structure can be classified as a true diamondoid (Figure 1.3) [3].

1.1 Nomenclature

Before going further, we first define the diamondoid classification and nomenclature. As can be anticipated, von Baeyer’s IUPAC names for these polycyclic

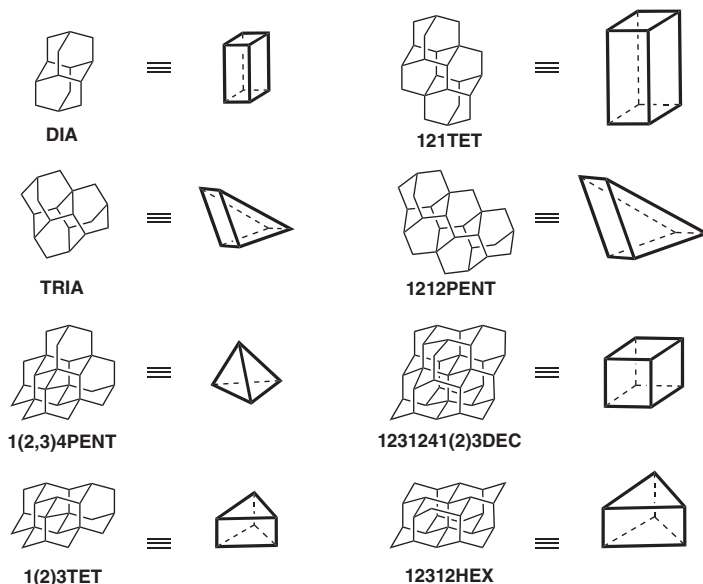


Figure 1.2 Structures of selected diamondoids linked to their geometrical representations. Source: Adapted from Ref. [5].

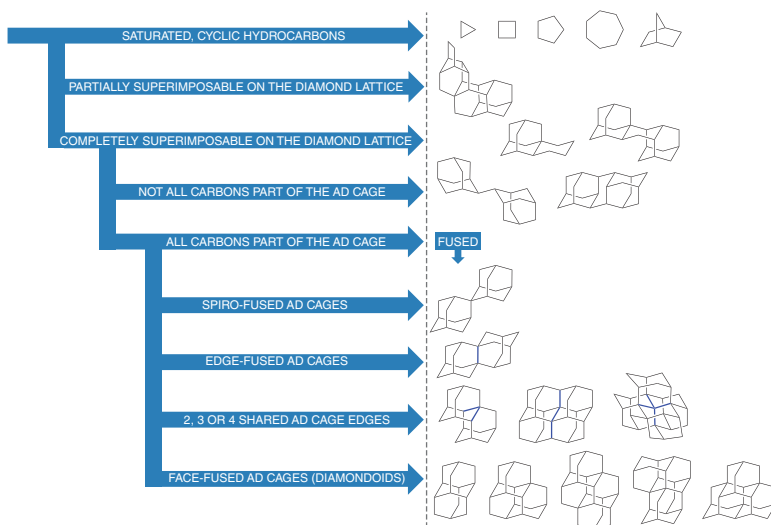


Figure 1.3 Classification of polyantmanes.

compounds become quite cumbersome, and precise structural assignments require representing such molecular structures in terms of planar graphs [6]. Note that some programs, such as ChemDoodle, are quite useful for automatic IUPAC naming. As the cages grow larger and become more complex, the need to develop a special nomenclature for diamondoids emerges [3]. The initially proposed

graph-theory-based diamondoid classification and nomenclature [7] is still in use today and is termed the Balaban–Schleyer nomenclature (vide infra). As for the naming, the smallest representative **AD** is the basis: numerical multipliers indicate the number of fused **AD** subunits and are followed by adding the *-amantane* suffix, e.g., **DIA**, **TRIA**, and **TET**. Note, however, that starting from **TET** different isomers emerge, and they also need to be defined unambiguously. For this purpose, a dualist graph construction is used that gives the codes for specific stereoisomers and avoids confusing and non-systematic designations. For example, three possible isomers of **TET** are sometimes called *anti-TET* (C_{2h} -symmetry), *skew-TET* (chiral, enantiomeric pair, and C_2 -symmetry), and *iso-TET* (C_{3v} -symmetry). However, this naming is based on their apparent geometrical shape and can hardly be transferred to higher homologues. In contrast, when applying the dualist graph convention, the naming becomes **121TET** (former *anti*, now [121]tetramantane), **123TET** (former *skew*, now [123]tetramantane), and **1(2)3TET** (former *iso*, now [1(2)3]tetramantane) and is a system applicable for all cage sizes. Essentially, this Balaban–Schleyer system uses four-digit codes (1, 2, 3, and 4) for the tetrahedral directions of covalent bonds around an imaginary center (Figure 1.4). These code descriptors are generated as follows: the center of the first **AD** cage is connected with the adjacent **AD** moieties in one of the four possible directions (**AD** has four faces), center-to-center. This direction is assigned number 1; the process is repeated until all **AD** subunits are accounted for and the whole molecule is traced with such vectors.

The digits emerge from taking different directions along the cage scaffold and, in the end, give a unique code characteristic for the isomer in question. This code is placed in brackets before the name of the stereoisomer. For more complicated geometries, when the diamondoid structure contains a branch, the digit of the corresponding vector is placed in parentheses, and if there are more branches, they are separated by commas inside the parentheses. In the case of longer branches, the chains of the branch are placed inside parentheses but without comma separation. One immediately notices the elegance of the Balaban–Schleyer approach as we have [123]tetramantane (**123TET**) instead of nonacyclo [11.8.1.0^{1,20}.0^{2,7}.0^{4,21}.0^{6,19}.0^{9,18}.0^{11,16}.0^{15,20}]docosane, [121]tetramantane (**121TET**)

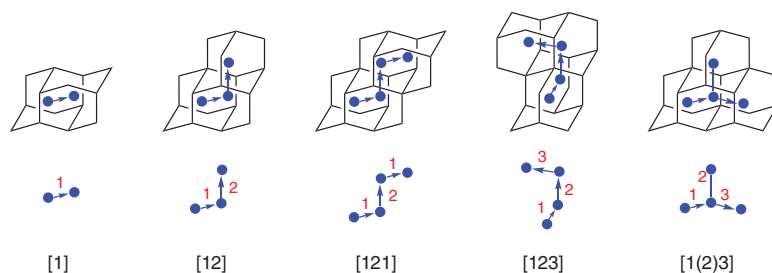


Figure 1.4 Examples of dualist graph construction for diamondoid naming suggested by Balaban and Schleyer.

instead of nonacyclo[11.7.1.1^{6,18}.0^{1,16}.0^{2,11}.0^{3,8}.0^{4,19}.0^{8,17}.0^{10,15}]docosane, [1212]pentamantane (**1212PENT**) instead of undecacyclo[11.11.1.1^{5,21}.0^{1,16}.0^{2,11}.0^{3,8}.0^{4,23}.0^{6,19}.0^{8,17}.0^{10,15}.0^{18,23}]hexacosane, and so on. Note that in the older literature, **DIA** is sometimes called “congressane” since it was proposed [8] as a synthetic challenge for the participants of the XIXth 1963 IUPAC meeting in London.

The dualist graph convention for the nomenclature of diamondoids enables a more straightforward way to designate diamondoid cages but as the cage size increases even such a naming system encounters complications. With increasing cage fusion, it becomes difficult to account for all possible stereoisomers and one way to resolve this type of complexity is to generate partitioned-formula tables based on the distribution of all the present carbon atoms according to them being quaternary (Q), tertiary (T), or secondary (S) [7a, 9]. By following this procedure, one obtains valence isomers of the same molecular formula $C_Q(CH)_T(CH_2)_S$ that are then shortened and denoted as Q–T–S, where the total amount of carbons is $C = Q + T + S$. For example, by using this convention, the formula for **AD** can be written as $(CH)_4(CH_2)_6$ or as 0–4–6, since the **AD** cage possesses no quaternary, four tertiary, and six secondary carbon atoms. Isomeric diamondoids with the same molecular formula, $C_Q(CH)_T(CH_2)_S$, can be divided into valence isomers by partitioning the number C into Q + T + S. Each [n]diamondoid has a dualist with n vertices and edges connecting vertices of adjacent **AD** units. Such a dualist is characterized by a quadruplet of indices (denoted as p, s, t, and q for primary, secondary, tertiary, and quaternary, respectively) specifying the connectivity of each vertex by assimilating it with a virtual carbon atom. Dualists help in classifying diamondoids as catamantanes with acyclic dualists, perimantanes with dualists having chair-shaped six-membered rings, or coronamantanes with dualists having only higher-membered rings.

An extension of the Schleyer–Balaban nomenclature that is more feasible for computer modeling was suggested recently [10]. This nomenclature is based on the numbering of centers of the diamond lattice starting from the origin (yellow, Figure 1.5) with further expansion along the chains and branches so that the structures can be systematically constructed. For instance, in accordance with this nomenclature, higher diamondoids [12312]hexamantane ($C_{26}H_{30}$), [121321]heptamantane ($C_{30}H_{34}$), and ([1 231 241(2)3]decamantane ($C_{35}H_{36}$) are now [1,2,3,6,7,18], [1,2,3,4,8,9,17], and [1,2,3,6,7,8,9,18,30] diamondoids that simplifies distinguishing and screening of large isomeric structures.

1.2 Strain

Strain reflects the electronic properties, and very recently it was found that the broad σ^*_{C-C} resonances in the near-edge X-ray absorption fine structure spectra of **AD** split into two narrow and intense resonances proportionally to the strain in a series from twistane and octahedrane to cubane [11]. It is often assumed that diamondoids are almost strain-free molecules, and indeed they are the most stable hydrocarbons of given brutto formulae. Strain can be seen as a relationship between

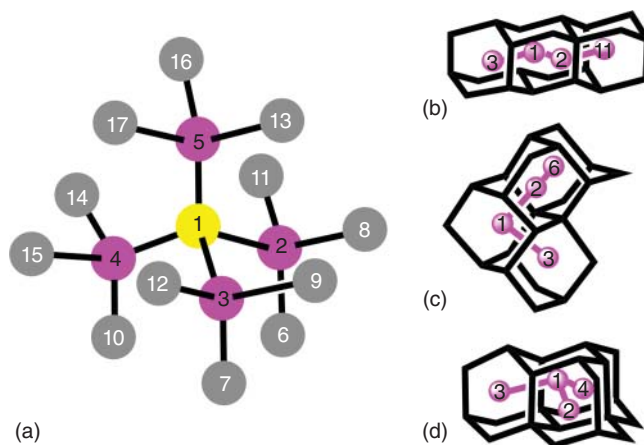


Figure 1.5 Nomenclature of diamondoids. (a) Parts of the diamond lattice with labeled numbers where the yellow atom represents the original atom and magenta and gray atoms are its first and second adjacent atoms, respectively; (b)–(d) are tetramantane isomers with numbering of their corresponding center atoms.

energy and structure that enables the evaluation of the structural feasibility of compounds. Straight-chain hydrocarbons in their linear, non-staggered conformations serve as the structural basis upon which strain is evaluated. Note, however, that even alkanes need not be absolutely strain-free but rather are taken as a point of reference for strain comparisons. Common criteria used when determining strain in structures are the presence of bond angles markedly deviating from the standard values, eclipsed conformations present in the structures, and atoms that approach each other too closely. Since the **AD** cage does not have these indicative features, it has long been considered strain-free (even though one should not forget about cyclohexane *gauche* interactions that lead to small strain, *vide infra*). While it is certainly true that diamondoids have little strain, there are some nuances to consider. Schleyer recommended using CH_3 , CH_2 , CH , and C group increments as well as force field calculations [12] for strain energy evaluations, in particular for diamondoids (Table 1.1) [13]. He concluded that the primary source of strain in diamondoids arises from slight deviations from the ideal C-C-C , C-C-H , and H-C-H angles when considering the cage angles where $\text{C-CH}_2\text{-C}$ and C-CH-C fragments are interconnected. For instance, while the C-C-C angles in **AD** are 109.5° , these values are 112.4° and 111.3° in propane and isobutane, respectively. With size growing, the strain energy of diamondoids increases: it amounts to ca. 6 kcal mol^{-1} for **AD**, 11 and 13 kcal mol^{-1} for **DIA** and **TRIA**, respectively. However, the normalized strain energy (per carbon) remains almost constant (*vide infra*). Another source of strain is repulsive nonbonding $\text{C}\cdots\text{C}$ interactions (akin to *gauche* interactions in *synclinal n*-butane and cyclohexane) throughout the cage itself. However, we also stress that 1,3-nonbonding intramolecular $\text{H}\cdots\text{H}$ interactions are in fact acting beneficially due to London dispersion [14] (rediscovered much later as “protobranching” [15]) that is seen as an interplay

Table 1.1 Computed enthalpies of formation (gas) and strain energies (E_{str}) in kcal mol⁻¹ for selected saturated hydrocarbons from molecular mechanics computations (EAS force field [12]).

Hydrocarbon	ΔH_f°	E_{str}
AD	-32.5	6.9
DIA	-37.4	10.7
TRIA	-44.4	13.4
Cyclopentane	-18.4	7.3
Cyclohexane	-29.4	1.4
Cycloheptane	-28.3	7.6
Cyclooctane	-29.2	11.9
Cyclononane	-30.7	15.5
Cyclodecane	-34.9	16.4
Norbornane	-13.0	17.0
ADAD	-53.7	21.5
Twistane	-13.3	26.1
Dodecahedrane	-0.2	43.0
Cubane	148.6	165.9

between medium-range correlation and steric repulsion [16]. The enthalpies of formation and evaluated strain energies for selected hydrocarbons presented in Table 1.1 are illustrative of the strain propagation in different cage molecules and are numerically still relevant [17] despite initially being computed using a simple Engler-Andose-Schleyer (EAS) force field method [12].

While the computational group equivalent approach is method-dependent [18], the errors largely cancel if homodesmotic equations are used [19]. The latter allows to compute the strain energies of hydrocarbons directly utilizing conventional strain-free references, such as ethane, propane, isobutane, and neopentane. This again gives the E_{str} of ca. 6 kcal mol⁻¹ for **AD** (Eq. 1.1) and 2.2 kcal mol⁻¹ for 1,3,5,7-tetramethyladamantane (**TMAD**) (Eq. 1.2) [15]. The fact that formally less crowded **AD** is more strained than **TMAD** may also be associated with additional electron delocalizations due to CC $\sigma \rightarrow \sigma^*$ hyperconjugation in the latter [20].

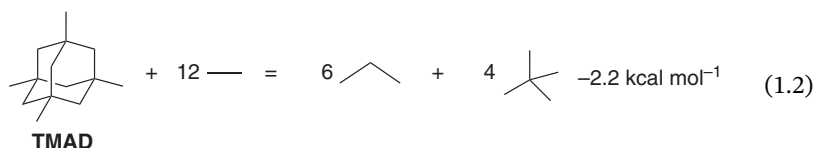
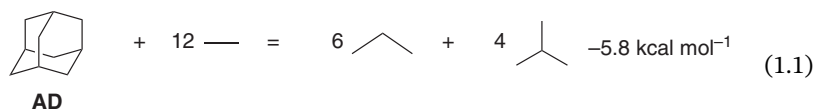


Table 1.2 Absolute (E_{str}) and normalized (per one carbon atom, E_{str}°) strain energies in kcal mol⁻¹ of selected diamondoids $C_{4n+6}H_{4n+12}$ evaluated through homodesmotic equation $C_{4n+6}H_{4n+12} + k H_3CCH_3 = l H_3CCH_2CH_3 + m (CH_3)_3CH + p (CH_3)_4C$ at the B3LYP/6-31G(d) level (Source: From [21]).

Diamondoid	E_{str}	E_{str}°
AD	6.0	0.60
DIA	9.1	0.63
TRIA	10.8	0.60
121TET	12.3	0.56
1(2)3TET	11.5	0.52
123TET	17.5	0.79
1(2,3)4PENT	9.3	0.36
12312HEX	16.2	0.62

Computations predict [10, 21] the lowest values of the formation enthalpies for the most symmetric diamondoid structures. Accordingly, C_{3v} -tetramantane (**1(2)3TET**) and T_d -pentamantane (**1(2,3)4PENT**) are the most stable isomers. The strain energies of higher diamondoids were calculated utilizing Eq. 1.1, namely, $C_{4n+6}H_{4n+12} + k H_3CCH_3 = l H_3CCH_2CH_3 + m (CH_3)_3CH + p (CH_3)_4C$ at the B3LYP/6-31G(d) level [21]. The calculated strain energy of **DIA** (9.1 kcal mol⁻¹) and **TRIA** (10.8 kcal mol⁻¹) is higher than that for **AD** (6.0 kcal mol⁻¹); however, the normalized values (E_{str}°) are virtually identical to that of **AD** (ca. 0.6 kcal mol⁻¹, Table 1.2).

Additional strain in higher diamondoids may arise from destabilizing transannular HH contacts, such as in **123TET**, where some distances are ca. 2.1–2.2 Å (Figure 1.6); these are shorter than the sum of the van der Waals radii of two H-atoms (ca. 2.4 Å) [22], which causes destabilization of the structure. Such interactions are not present in **121TET** and **1(2)3TET**, which almost level their strain energies. Note that while the ideal tetrahedral **1(2,3)4PENT** is almost strain-free (0.36 kcal mol⁻¹ per carbon), the strain energy of **12312HEX** (0.62 kcal mol⁻¹ per carbon) is close to that of **AD**.

1.3 Preparation of Diamondoids

The construction of the **AD** core in tetraester (**TE**) was first achieved in 1937 by Oskar Böttger [23] through methylenation of Meerwein's ester (**ME**, Scheme 1.1) [24], readily available from formaldehyde and malonic ester [25]. The first successful synthesis of **AD** was achieved by Prelog [24, 26] as early as 1941, starting from **ME** through diester (**DE**) [27], however, with a very low yield (0.16% based on

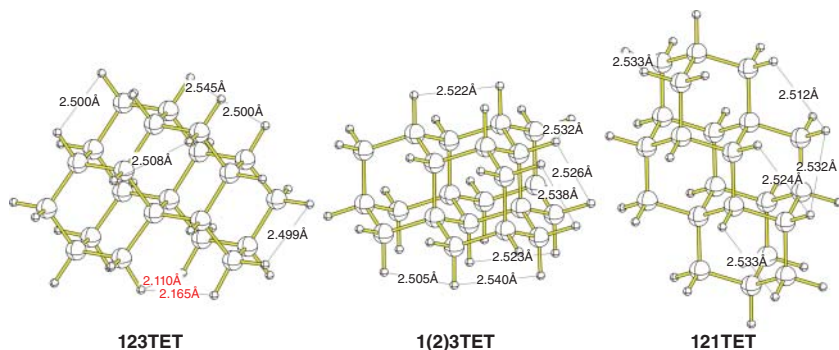
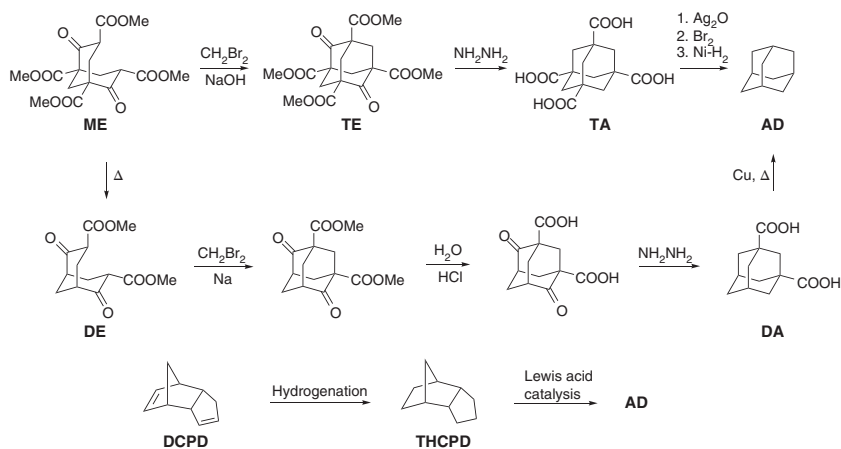


Figure 1.6 Additional strain in the skew-diamondoid **123TET** arose from several destabilizing transannular HH contacts (in red). The 1,3-HH contact distances of 2.5 Å are close to the sum of the van der Waals radii of two H-atoms (ca. 2.4 Å) and are stabilizing (protobranching).

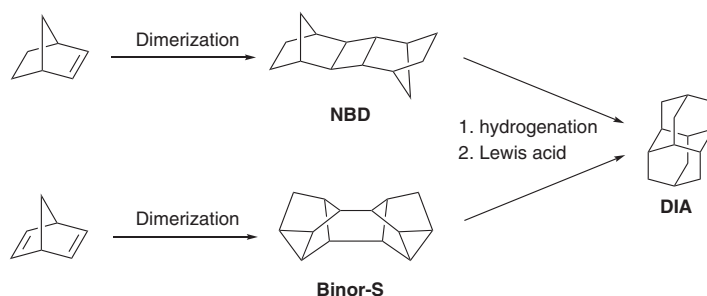
ME). Further improvements of the decarboxylation steps, either through reductive decarboxylation of diacid **DA** [28] or tetraacid **TA** [29], utilizing the Hunsdiecker reaction, allowed for an increase in the overall yield of **AD** up to 1.5 and 6.5%, respectively. The bottleneck is the methylenation of **ME**, which determines the generally low yields. Schleyer, one of the most influential organic chemists of the twentieth century, simplified and perfected the synthesis of **AD** [30], making it available on an unprecedented large scale [31]. Schleyer's synthesis (Scheme 1.1, bottom) is based on the thermodynamically favorable Lewis acid-catalyzed rearrangement of tetrahydrodicyclopentadiene (**THCPD**) to **AD** [32]. Such "stabilomeric synthesis" not only made **AD** available in large quantities and thus significantly promoted the



Scheme 1.1 Final steps in the synthesis of **AD** from Meerwein's ester (**ME**, top) and improved Schleyer's synthesis of **AD** from dicyclopentadiene (**DCPD**, bottom) through hydrogenation to tetrahydrodicyclopentadiene (**THCPD**) followed by Lewis acid-catalyzed rearrangement.

chemistry of cage compounds but also became very useful for the synthesis of larger polymantanes (vide infra).

The second diamondoid homologue, **DIA**, is also available synthetically and was first prepared by Schleyer and Cupas applying the same Lewis acid-catalyzed rearrangement procedure [8]. Photodimerization of norbornene afforded a cyclobutane-containing dimer **NBD**, which was treated with AlCl_3 and gave **DIA** (Scheme 1.2). As Schleyer noted [33], “Although the four-membered ring ... was not ideal (too much strain in rearrangement precursors normally leads to ring opening and tar formation), I ... suggested to Chris Cupas that he investigate the rearrangement. The first experiment failed but in the second experiment he noticed sublimed crystals on the cooler portion of the flask that proved to be congressane.” This method unfortunately gave very low yields and produced a significant amount of tar, although it enabled X-ray analysis and confirmation of the **DIA** structure [34]. Schleyer further improved the synthesis to make it relevant for practical applications [35]. The modification included the use of a more efficient precursor, **Binor-S** [36], that, after hydrogenation and treatment with AlBr_3 , gave **DIA** in a yield of over 60% for the last step (Scheme 1.2) [35, 37].



Scheme 1.2 First synthesis of **DIA** from the norbornene dimer (**NBD**) and multi-gram synthesis using **Binor-S** as a precursor.

Schleyer also prepared **TRIA** in a similar way from bis-cyclopropanated polycyclic dimer of cyclooctatetraene (**DCOT**) using the AlBr_3 /*tert*-BuBr sludge catalyst [38]. Reductive cleavage of the cyclopropane rings followed by isomerization resulted in **TRIA**, albeit in a very low yield (under 5%) for the final step. McKervey made a slight improvement in **TRIA** synthesis by using **1COOHDIA** as a starting molecule that underwent cage rearrangement as the last step [39], and he could further improve the synthesis by using **Binor-S** heated on a platinum catalyst that gave cyclic olefins [40]. Diels–Alder reaction of these olefins with butadiene and Lewis acid-catalyzed rearrangement afforded the target hydrocarbon with satisfactory preparative yield (Scheme 1.3).

The attempt to expand the stabilomeric approach to the preparation of diamondoids higher than **TRIA** failed. In particular, the isomerization of $\text{C}_{22}\text{H}_{28}$ hydrocarbons derived from the hydrogenation of the Diels–Alder adduct of 1,3-cyclohexadiene with the 38.5 °C melting cyclooctatetraene dimer (**DCOT**) gave unwanted ethano-bridged isomer “bastardane” (**BAST**) rather than **121TET**